Mater. Res. Soc. Symp. Proc. Vol. 1206 © 2010 Materials Research Society 1206-M11-42

Catalyst-Free GaN Nanowire Nucleation: Correlation of Temperature-Dependent Nanowire Orientation and Growth Matrix Changes

Kaylee McElroy[1], Virginia M. Ayres[1], Thomas R. Bieler[1], Benjamin W. Jacobs[1,2], Martin A. Crimp[1]

[1]College of Engineering, Michigan State University, East Lansing, MI 48824-1226, U.S.A.

[2]Present address: Sandia National Laboratories, Livermore, CA 94551-0969, U.S.A.

ABSTRACT

Growth orientation and type of internal structures are both observed to change abruptly as a function of growth temperature in catalyst free growth of gallium nitride nanowires. In the present work, corresponding temperature-dependent changes in the growth matrix substrate that can affect the availability of nucleation sites and influence the reactivity of constituent adatom materials in catalyst-free nanowire growth are investigated. The influence of Ga vapor pressure and an abrupt change in the availability of single versus molecular adatom constituents is identified as a possible controlling parameter.

INTRODUCTION

Gallium nitride (GaN) nanowires have been under extensive investigation in recent years due to their unique optical [1] and electrical properties [2] as well as their potential advantages in enabling new device applications [3, 4]. For device applications, control of crystalline quality and orientation is essential. To develop controlled nanowire growth processes, it is critical to understand nanowire nucleation and growth mechanisms.

The nanowires examined in this study were grown using a catalyst-free growth method [5] at furnace growth temperatures of 850°C, 950°C and 1000°C. Catalyst free nanowire growth [5,6,7,8] results in no metal impurities in the nanowires and can be used in applications where device fabrication steps are incompatible with the presence of a metal catalyst [9, 10]. In previously reported work [11,12,13], we demonstrated that the nanowire growth orientation was influenced by growth temperature. Between 950°C to 1000°C, an abrupt change in wurtzite growth orientation from $\langle 11\bar{2}0 \rangle$ to $\langle 0001 \rangle$ is observed. We further reported that the GaN nanowires had internal structures that continued along the entire length of the nanowires. The majority of nanowires grown at 850°C and 950°C had multiphase wurtzite and zinc-blende crystalline domains that persisted along the entire nanowire length. The growth direction was $\langle 110 \rangle$ for the zinc-blende domains and $\langle 11\bar{2}0 \rangle$ for the wurtzite domains as stated. Very recently, zinc-blende/wurtzite multi-domain GaN nanowires have been reported by another group [14]. In contrast, the majority of nanowires and rods grown at 1000˚C were single-phase wurtzite with a $\langle 0001 \rangle$ growth orientation and a different internal structure consisting of a single nanopipe [13]. A nanopipe can develop from relaxation of a large Burgers vector screw dislocation [15]. While

ours is the first reported observation of nanopipe formation in the GaN nanowire system, evidence for formation of an internal screw dislocation in the related PbS nanowire system has been reported by another group [16].

In the present work we identify corresponding temperature-dependent changes in the growth matrix substrate. These changes in the growth matrix substrate have a direct effect on the availability of nucleation sites and subsequent catalyst-free growth of nanowires with the observed orientations and internal structures.

EXPERIMENTAL DETAILS

Preparation of samples

The GaN nanowires nucleated on a polycrystalline growth matrix, whose formation preceded the onset of nanowire growth. Details of the growth conditions in a quartz tube furnace correlated with flow rate and temperature are given in Ref. [5]. TEM [12] and X-ray diffraction [17] to date have found only wurtzite growth matrix with no evidence of zinc-blende.

Experimental results

The top, bottom and side (fracture cross section) surfaces of 850°C, 950°C and 1000°C growth matrix samples were characterized using scanning electron microscopy (SEM) using a Hitachi S-4700- II FESEM. The growth matrix morphology was observed to change as a function of growth temperature. The 850°C and 950°C growth matrix crystallite formations were similar. The top surface consisted of approximately 1μm-sized crystallites. Nanowires with triangular cross-section widths ranging from 50nm to 250nm were observed to grow from the top surfaces of the 850°C and 950°C growth matrix samples. Figure 1 (a) is a side view image that also shows the sub-surface of the growth matrix near the top. A hexagonal platelet morphology was observed (close-up shown in inset)

At 1000°C, three different crystallite formations were typically observed at the top surface of the growth matrix. Type 1 (top of figure 1 (b)) consisted of relatively large 1-20μm crystallites of GaN. A hexagonal block morphology was typically observed for the large crystallites (close-up shown in inset). Large hexagonal rods, with widths ranging from 0.5μm to 30μm, grew from the Type 1 matrix. TEM confirmed that the rods had ⟨0001⟩ growth orientation. Type 2 (bottom left) consisted of medium sized 0.1-1μm crystallites. The Type 2 growth matrix at 1000°C appeared to be comparable to the 850°C and 950°C

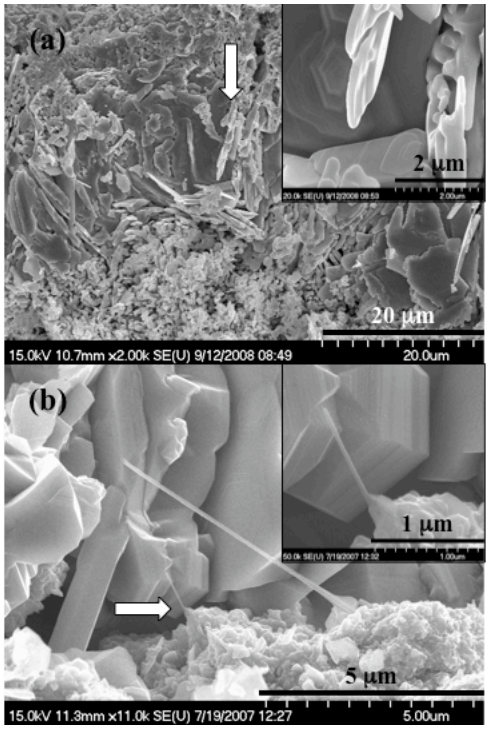

Figure 1. SEM images of different morphologies of (a) 850˚C GaN growth matrix (side view and top surface) and (b) 1000˚C GaN growth matrix (top view). Arrows mark areas shown at higher magnification in insets.

growth matrix and also nucleated similar nanowires, with no rods observed. Type 3 (bottom right) consisted of small 50-300 nm crystallites typically clustered in spherical mounds. Nanowire growth was also observed from Type 3 growth matrix. The nanowires that nucleated from Type 2 and 3 matrixes at 1000°C had triangular cross sections associated with $\langle 11\bar{2}0 \rangle$ wurtzite-phase orientation [12] in nanowires that nucleated from 850°C and 950°C matrix samples.

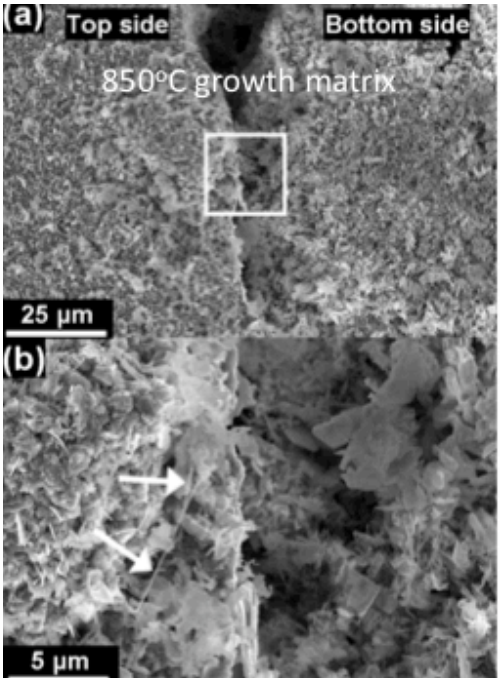

Figure 2. (a) Matrix morphologies of the top and bottom surfaces of the 850°C matrix were similar. (b) High magnification image of the boxed area in (a). Arrows point to nanowires on the top surface (left). No nanowires were observed on the bottom surface (right).

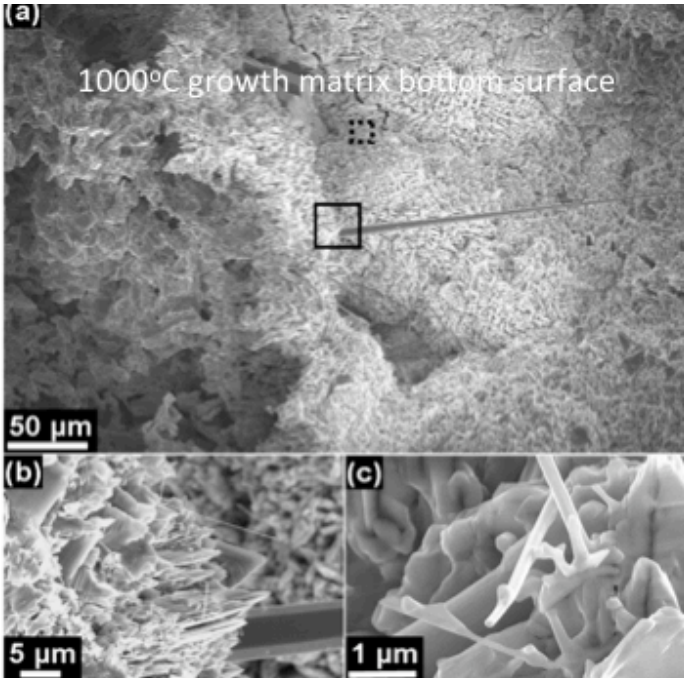

Figure 3. (a) A low magnification image of the bottom surface of the 1000°C growth surfaces. A close-up of the area in the solid square is shown in (b), showing nanowire growth near the base of a rod. A close-up of the area in the dotted square in (c) shows possible dendritic nanowire growth.

The bottom of the growth matrix (the side that formed on the quartz tube in the growth furnace) was also imaged using SEM to study the evolution of the matrix. In figure 2, the top and bottom sides of two pieces of matrix from the 850°C growth are shown side-by-side. In figure 2 (a), the morphologies of the matrix on both surfaces appeared similar, however, nanowire nucleation was only observed on the top surface of the matrix, as shown in figure 2 (b). The top and bottom of the 950°C growth matrix were similar, with nanowire growth observed only on the top surfaces. In contrast, the bottom surface of the 1000°C growth matrix was as active in nanowire nucleation as the top surface. A low magnification image of the bottom surface of a 1000°C growth matrix sample is shown in figure 3 (a) with rod growth apparent. A close-up of the area at the base of one rod (solid box) in figure 3 (b) shows that nanowire nucleation was also present. Nanowires were observed to nucleate from areas of the matrix with smaller crystallites,

while the rod nucleation sites were 'buried' in a growth of smaller crystallites. A close-up of a different point on the same sample (dotted box) in figure 3 (c) shows that some nanowires display nodules and branching. This morphology indicated the onset of dendritic growth.

DISCUSSION

The results clearly indicate that a temperature-dependent change in the growth matrix is observed between 950°C and 1000°C, which parallels the temperature-dependent changes in the nanowire orientation and internal structure. The initial growth and evolution of the growth matrix is first considered. Briefly summarizing the results reported in Ref. [5], at the initial vapor pressure of about 0.05 Torr at room temperature solid gallium diffuses to form an initial liquid layer on the fused silica wall of the tube furnace growth chamber, which then oxidizes to Ga_2O_3. Ammonia flow was then introduced and the furnace temperature was subsequently brought up to the growth temperature, which increased the vapor pressure of Ga.

The temperature dependent equilibrium of Ga and Ga_2O_3 can be related to the equilibrium ratio of hydrogen to water vapor, p_{H2}/p_{H2O}, which is > ~10^6 in the experimental temperature range [18]. This critical ratio is achieved by introducing hydrogen by two events. Cracking of NH_3 will occur with increasing temperature. When H_2 is supplied, the Ga_2O_3 layer reverts to a clean Ga layer, with a transient increase in H_2O. Decomposition of NH_3 by the clean Ga layer will generate hydrogen by a second mechanism. This presence of hydrogen creates a reducing environment that eliminates Ga_2O_3, freeing the Ga to react with N.

The transition in growth matrix morphology with temperature indicates a change in growth environment and mechanism. Given that the ammonia flow rate provided a pressure of 0.15 Torr, the ambient NH_3 pressure in the tube was several orders of magnitude greater than the Ga vapor pressure, indicating that the environment was supersaturated with N for all three temperatures. The Ga vapor pressure is a strong function of temperature, based upon the thermodynamic equilibrium of the vapor and condensed phases:

$$\mathrm{Log}(p) = (A/T) + B\ \log(T) + C \qquad (1)$$

where A, B, and C are constants found in standard thermodynamic reference tables and temperature T is in K. The calculated Ga vapor pressure, normalized to p(850°C), is given as a function of temperature in Table I. This shows that there were 10 times as many Ga atoms present in the plasma at 950°C than at 850°C and 30 times as many at 1000°C than at 850°C.

Table I. Ga vapor pressure as a function of temperature normalized to p(850°C).

Temperature °C	Log p	p, Torr	p/p(850°C)
850	-4.545	2.85E-05	1.00
950	-3.493	3.21E-04	11.27
1000	-3.030	9.33E-04	32.75

It would be generally expected that crystal growth would occur at a greater rate with both an increase in temperature and/or an increase in Ga vapor pressure. Nevertheless, the observation that the growth matrix morphology is substantially different at 1000°C suggests that the growth mechanism was different from what occurred at lower temperatures. A possible high

temperature growth mechanism is that N and Ga react in the gaseous phase to form GaN molecules, which subsequently attach to a growth surface, leading to equiaxed growth. Molecular growth is consistent with large equiaxed crystals because GaN molecules can attach to any location on an initial nucleus. Rapid growth is further encouraged by the self-orientation of the arriving GaN molecules due to their polarity. The molecular growth mechanism is consistent with the large blocky growth matrix crystallites observed at 1000°C (figure 1 (b) inset).

The large blocky growth matrix morphology that forms at 1000°C has a direct effect on the internal structure and orientation of the rods and nanowires that nucleate at this temperature. As the growth matrix crystallites increase in size, the statistical probability of forming screw dislocations increases. Our observations of nanopipes [13] in (0001) oriented hexagonal cross section rods and nanowires grown at 1000°C indicate the presence of axial screw dislocations. This is consistent with a nucleating growth matrix that contains screw dislocations and a rod/nanowire growth mechanism based upon spiral growth about a screw dislocation ledge.

At 850°C and 950°C, the growth matrix morphology is platelet rather than blocky (figure 1 (a)). This implies that growth along the platelet edges is faster than growth on the basal plane surface (the basal plane is implied by the hexagonal platelet shape and confirmed by TEM [12]). The lower temperature, coupled with the lower Ga vapor pressure, reduced the likelihood of forming GaN molecules in the plasma. This suggests that the rate-limiting step is arrival of single Ga atoms. Step-ledge growth on platelet edges is therefore a likely platelet growth mechanism. The faster growth rate on edges is correlated with a higher surface energy (i.e. a higher capture efficiency) than on the basal plane, and the fact that there are sites available for both Ga and N atoms. Furthermore, single adatom matrix crystallite growth provides opportunities for 'wrong' additions. To form a zinc-blende nucleus on a wurtzite GaN substrate only requires putting a Ga atom into an alternative stacking position between wurtzite N atoms. If this occurred in enough places to establish a zinc-blende nucleus, this may facilitate growth of a zinc-blende domain. This possibility is supported by the observation that nanowires grown at 850°C and 950°C were multi-domain zinc-blende/wurtzite with the zinc-blende nanowire growth axis perpendicular to the basal plane normal. Furthermore, the thin platelet size also reduces the possibility for the formation of crystallites large enough to generate screw dislocations, indicating that (0001) oriented nanowire growth perpendicular to the basal plane is not favorable at lower temperatures.

CONCLUSIONS

In catalyst free growth of gallium nitride nanowires, the growth orientation and type of internal structures were both observed to change abruptly as a function of growth temperature. Corresponding temperature-dependent changes in the wurtzite growth matrix, from thin hexagonal platelets to large hexagonal blocks, were demonstrated. An abrupt change in the availability of single versus molecular adatom constituents as a function of Ga vapor pressure is identified as a possible controlling parameter. Large block versus platelet growth matrix morphologies are consistent with the availability of screw dislocation versus step ledge nucleation sites that correlate with the observed nanowire and rod growth orientations.

ACKNOWLEDGEMENTS

The support of NASA Goddard Space Flight Center, MEI Task No. 14, and National Science Foundation IREE grant DMI-0637134, is gratefully acknowledged. One author (B.W.J.) thanks the NASA Graduate Student Researchers Program. The authors thank Maoqi He and Joshua B. Halpern of Howard University for sourcing the nanowires used in this study.

REFERENCES

1. J. Johnson, H. Choi, K. Knutsen, R Schaller, P. Yang, and R. Saykally, *Nature Mater.* **1**, 106 (2002).
2. B. W. Jacobs, V. M. Ayres, R. E. Stallcup, A. Hartman, M. A. Tupta, A. D. Baczewski, M. A. Crimp, J. B. Halpern, M. He, and H. C. Shaw, *Nanotech.* **18**, 475710 (2007).
3. Y. Huang, X. Duan, Y. Cui, and C. Lieber, *Nano Lett.* **1**, 6 (2002).
4. Y. Huang, X. Duan, and C. Lieber, *Small* **1**, 142 (2005).
5. M. He, P. Zhou, S. Mohammad, G. Harris, J. B. Halpern, R. Jacobs, W. Sarney, and L. Salamanca-Riba, *J. Cryst. Growth*, **231**, 357 (2001).
6. E. Calleja, M. A. Sanchez-Garcia, F. J. Sanchez, F. Calle, F. B. Naranjo, E. Munoz, S. I. Molina, A. M. Sanchez, F. J. Pacheco, and R. Garcıa, *J. Cryst. Growth* **296**, 201 (1999).
7. M. Yoshizawa, A. Kikuchi, M. Mori, N. Fujita, and K. Kishino, *Jpn. J. Appl. Phys.* **36**, L459 (1997).
8. T. Stoica, E. Sutter, R. Meijers, R. K. Debnath, R. Calarco, and H. Luth, *Small* **4**, 751 (2008).
9. M. Heiß, A. Gustafsson, S. Conesa-Bo j, F. Peiro, J. Morante, G. Abstreiter, J. Arbiol, L. Samuelson, and A. Fontcuberta i Morral, *Nanotech.* **20**, 075603 (2009).
10. C. Thelander, P. Agarwal, S. Brongersma, J. Eymery, L. F. Feiner, A. Forchel, M. Scheffler, W. Riess, B. J. Ohlsson, U. Gosele and L. Samuelson, *Mater. Today* **9**, 28 (2006).
11. B. W. Jacobs, V. M. Ayres, M. P. Petkov, J. B. Halpern, M. He, A. D. Baczewski, K. McElroy, M. A. Crimp, J. Zhang, H. C. Shaw, *Nano Lett.* **7**, 1435 (2007).
12. B. W. Jacobs, V. M. Ayres, M. A. Crimp, and K. McElroy, *Nanotech.***19**, 405706 (2008).
13. B. W. Jacobs, M. A. Crimp, K. McElroy, and V. M. Ayres, *Nano Lett.* **8**, 4353 (2008).
14. H. Y. Xu, Z. Liu, Y. Liang, Y. Y. Rao, X. T. Zhang, and S. K. Hark, *Appl. Phys. Lett.* **95**, 133108 (2009).
15. F. C. Frank, *Acta Cryst.* **4**, 497 (1951).
16. M. J. Bierman, Y. K. A. Lau, A. V. Kvit, A. L. Schmitt, and S. Jin, *Science* **320**, 1060 (2008).
17. K. McElroy, *Catalyst-free Gallium Nitride Nanowire Nucleation*, Thesis for Master of Science in Electrical Engineering, Michigan State University, 2009.
18. D. R. Gaskell, *Introduction to the Thermodynamics of Materials*, 5th edition (Taylor & Francis, New York, NY, 2008).